The Comparison of pH Sensing Performance Based on Different Polymer Materials of TiO₂-Based Electrode

Aina Syakirah Mohd Masri, Nur Syahirah Kamarozaman, Nurbaya Zainal, Zurita Zulkifli* and Sukreen Hana Herman

Abstract—This paper discussed on the comparison of pH sensor performance with different types of polyaniline (PANI) polymers as the TiO2 composite sensing electrode material. Two types of PANI polymer were employed in this experiment which known as PANI emeraldine base (EB) and emeraldine salt (ES). By incorporating PANI into the sensing layer, the conductivity, stability, and sensitivity of the overall sensor performance can be enhanced. The digital microscopy revealed TiO2-PANI EB's superior uniformity and dispersion compared to TiO2-PANI ES, which exhibited undissolved regions, indicative of their distinct solubility behaviours. FESEM analysis further exhibited identical surface morphology for both samples. TiO2-PANI EB's shows an excellent electrochemical sensing electrode with hydrophobic properties measured by contact angle 92.70°. EDX analysis showed that TiO2-PANI EB had a higher content of PANI material, resulting in higher conductivity and superior sensor response. TiO2-PANI EB's Nernst response exhibited higher sensitivity and linearity (57.10 mV/pH, 0.9995) compared to TiO₂-PANI ES (46.24 mV/pH, 0.9963). These findings underscore the critical impact of polymer selection on the interfacial properties and overall functionality of TiO2-PANI-based films pH sensors, providing significant insights for advancing sensor technologies in various applications.

Index Terms—EGFET, Nanocomposite, PANI, Spin Coating, TiO₂

I. INTRODUCTION

pH sensors are essential tools in various fields, including environmental monitoring, biomedical research, and industrial processes, where precise pH measurements are critical. The performance of pH sensors depends significantly on the

This manuscript is submitted on 22nd February 2025, revised on 29th May 2025, accepted on 13th October 2025 and published on 31st October 2025. Aina Syakirah Mohd Masri and are currently pursuing her PhD in Electrical Engineering, Faculty of Electrical Engineering, Universiti Teknologi MARA, 40450, Shah Alam, Selangor.

Nur Syahirah Kamarozaman and Nurbaya Zainal are with Faculty of Electrical Engineering, Universiti Teknologi MARA, 40450, Shah Alam, Selangor. Zurita Zulkifli is with Nano-ElecTronic Research Group, Faculty of Electrical Engineering, Universiti Teknologi MARA, 40450, Shah Alam, Selangor. Sukreen Hana Herman is with Microwave Research Institute, Universiti Teknologi MARA, 40450, Shah Alam, Selangor.

*Corresponding author Email address: zurita101@uitm.edu.my

1985-5389/@ 2023 The Authors. Published by UiTM Press. This is an open access article under the CC BY-NC-ND license (http://creativecommons.org/licenses/by-nc-nd/4.0/).

characteristics of their sensing layers, which directly interact with the surrounding electrolyte environment. Recent advancements in material science have led to the development of innovative composite materials for enhancing the performance and reliability of pH electrodes. An Extended-Gate Field-Effect Transistor (EGFET) is a sophisticated measurement setup widely used in sensor technology, especially for characterizing and evaluating pH sensor electrodes as evidenced by previous research [1-4]. This setup incorporates a gate electrode into the sensor system, enabling the assessment of the electrodes' precision in detecting and measuring pH variations, facilitated by the presence of hydrogen (H⁺) and hydroxide (OH⁻) ions in the environment. These ions play a crucial role in pH measurements, especially in aqueous solutions, where they contribute to the acidity or basicity of the solution.

One promising area of research is the integration of titanium dioxide (TiO₂) and polyaniline (PANI) composites in pH sensor electrodes. Recently, TiO₂ has gained attention in sensor development since it offers excellent chemical stability and catalytic properties, making it suitable for sensor applications [5-8]. For example, Cheng reported super-hydrophilic pH electrode, fabricated using a chemical etching method on a TiO₂ thin film, exhibited high sensitivity (54.13 mV/pH) in pH 4 - 12 [6]. In another study by Nematzadeh, TiO₂-coated spirals, grown via atomic layer deposition (ALD) at temperatures of 150°C and 300°C with thicknesses of 20, 40, and 80 nm, exhibit varied electrical and chemical properties affecting pH response and capacitance, with the 80 nm sample deposited at 300°C demonstrating the optimal pH response of 40 mV/pH [7].

Polyaniline, a conductive polymer, exhibits outstanding electrochemical properties that are ideal for use in electrode materials [9-10]. The integration of nanomaterials like TiO₂, carbon nanotubes (CNTs), and gold nanoparticles (AuNPs) into the PANI matrix holds promise for enhancing sensor performance, leveraging their unique physicochemical properties and synergistic effects to achieve superior sensing performance [11-13]. PANI, exists in three main oxidation states: leucoemeraldine base (LEB), emeraldine base (EB), and pernigraniline base (PB), each with unique electronic structures and conductivity levels [14]. Generally, the conductive form of polyaniline, emeraldine salt (PANI ES), is obtained by doping the insulating PANI EB with a protonic acid [15], and their performance as pH sensing electrodes was evaluated when

combined with a TiO2 solution. This study focuses on investigating and comparing the performance of pH sensor electrodes with sensing layers based on TiO₂-PANI composites, utilizing two different types of PANI; PANI (Emeraldine Base) and PANI (Emeraldine Salt). They were usually formed in different colours, with PANI EB appearing in blue and only becoming conductive when properly doped, resulting in the PANI ES form which appeared in light green. Recent research conducted by Qiao explored the potential of PANI EB as a highperformance cathode material for alkaline ion batteries (AIBs) compared to doped PANI, demonstrating excellent electrochemical performance and charging rate [16]. This material showed promise for reliable and stable electrochemical responses to changes in pH, suggesting enhanced accuracy in pH sensing capabilities, with the potential for improved sensitivity and response times through increased charging voltage. Furthermore, findings by Morsy indicated that the sensor performance of a PANI-Titania nanotube-rGO nanocomposite was improved by incorporating PANI EB through hydrothermal and in situ polymerization processes, leading to increased sensitivity and a faster response time, thus optimizing humidity sensing performance [17].

To comprehensively evaluate the pH sensor electrode performance composite TiO₂-PANI-based films by two variants polymer PANI EB and PANI ES, this study employs a multi-dimensional characterization approach, including digital microscope, Field Emission Scanning Electron Microscopy (FESEM) Contact Angle analysis, Energy Dispersive X-ray (EDX) spectroscopy and Nernst response analysis. By integrating these comprehensive analytical techniques, this study aims to elucidate the relationship between the material properties of composite TiO₂-PANI-based films, surface characteristics, and pH sensing performance, particularly focusing on the influence of different PANI types.

II. METHODOLOGY

The methodology part was structured into distinct phases aimed at accomplishing the primary objective. Fig. 1 presents a flowchart summarizing the methodological steps involved in the synthesis of TiO₂-PANI EB and TiO₂-PANI ES electrode, their deposition on ITO substrates using spin coating, subsequent characterization techniques. The importance of contact angle of the sensing electrode is essential to produce a highly sensitive pH sensor. The wettability of these films was assessed through contact angle measurements to evaluate their interfacial properties, which can classify the sensing electrode as hydrophilic or hydrophobic properties.

A. Sensing Electrode Preparation

The ITO substrate with dimensions of 1 cm x 2 cm was used and then sonicated using the methanol solution, followed by DI water to avoid any contamination before the deposition process started. The TiO₂ solution was prepared first using the optimized recipe. As for the TiO₂-PANI EB solution preparation, 50.25 ml of TiO₂ solution was mixed with 10 mg of PANI EB powder that had been diluted with 1 ml of dimethylformamide (DMF) [18-19]. The solution was stirred at

a speed of 400 rpm at room temperature for 1 hour. For the TiO₂-PANI ES solution preparation, 20 ml of TiO₂ solution was mixed with 10 mg of PANI ES powder that had been diluted with 9.99 ml of methanol. The solution was stirred at a speed of 400 rpm at room temperature for 15 minutes. TiO₂-PANI EB presented a darker green solution compared to TiO₂-PANI ES.

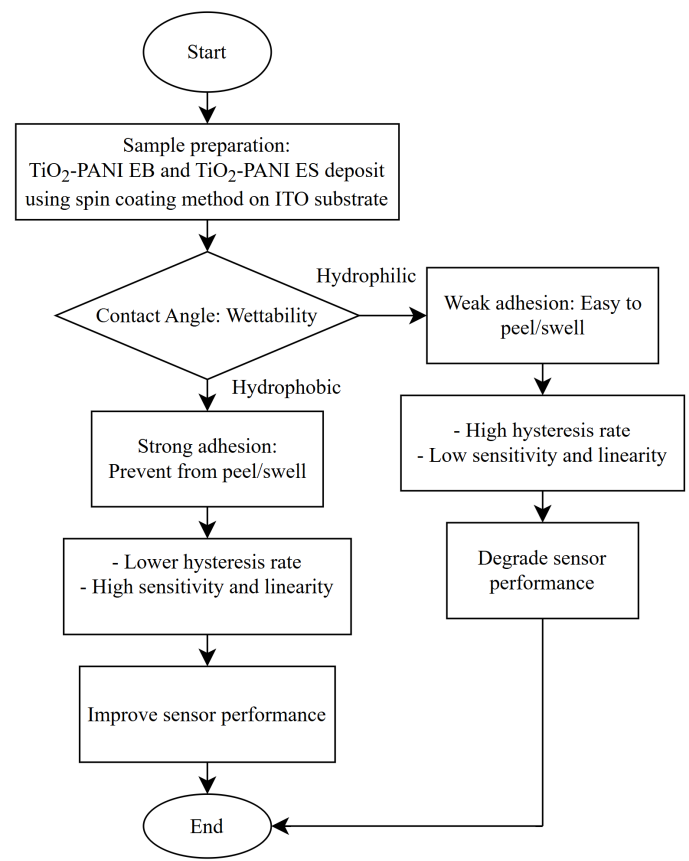


Fig. 1. Flowchart.

B. Deposition Process

The deposition process for both solutions, TiO₂-PANI EB and TiO₂-PANI ES were carried out using the spin coating method. Fig. 2 demonstrated the spin coating method, where the solution was dropped onto the surface of the ITO substrate while the substrate holder rotated. Table I shows the deposition parameters that were applied for each sample. All samples were then dried at 150°C for 10 min using the furnace.

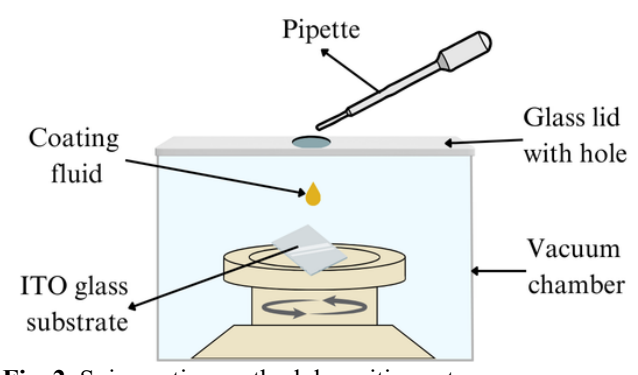


Fig. 2. Spin coating method deposition setup.

TABLE I. SPIN COATING METHOD DEPOSITION PARAMETERS

Deposition parameter	Constant parameter
Rotational speed	3000 rpm
Deposition rate	10 drop/min
Deposition time	1 min

C. Surface Morphology Characterization

The TiO₂-PANI EB and TiO₂-PANI ES were observed using the digital microscope OLYMPUS (U-MSSP4) with a magnification of 20x and FESEM at a magnification of 50,000x FESEM Thermo scientific Apreo 2 S. The specific surface structure were examine during the analysis.

D. Contact Angle

Wettability analysis on the deposited layer was performed using a contact angle measurement setup (VCA3000S) utilising a precision camera and advanced PC technology. The sessile drop of 3 μ L DI water was dispensed at three random areas to determine the interfacial properties of the sensing layer. The contact angle θ , which was formed between the droplet and the modified surface, served as the measurement of the surface's static wettability. The classifications for the three types of surfaces were as follows: hydrophilic when $\theta < 90^\circ$, hydrophobic when $\theta > 0^\circ < \theta < 150^\circ$ degrees, and superhydrophobic when $\theta > 150^\circ$ [20-23].

E. EDX Analysis

EDX was employed to analyze the chemical composition of TiO₂-PANI-based films. The percentage of TiO₂ and PANI distribution in specific areas was traced and confirmed to validate their atomic percentage presence.

F. Hysteresis Characteristic

The hysteresis characteristics of the sensing electrodes (SEs) were analyzed under cyclic pH conditions using an EGFET setup connected to B1500A measurement equipment. The acidic loop involved sequential pH transitions: $7 \rightarrow 4 \rightarrow 7 \rightarrow 10 \rightarrow 7$, completed over 25 minutes period. The TiO₂-PANI EB and TiO₂-PANI ES electrodes were subjected to this cyclic protocol to evaluate their hysteresis behavior. Voltage reference were recorded at each pH step, and the resulting hysteresis curves were used to assess the stability and performance of the electrodes under dynamic pH changes.

G. Nernst Response Analysis

Nernst response analysis was performed to evaluate the performance of the pH electrodes using the EGFET setup on the Keysight B1500A Semiconductor Device Analyzer. This study employed an EGFET analysis that involved measuring the electrode's response to changes in pH levels and determining its sensitivity and linearity in pH detection. The Nernst response was related to a 59 mV/pH change. This meant that for each tenfold increase in hydrogen ion concentration, there was a 59 mV shift in cell potential at room temperature [24]. The Nernst equation, which related the electrode potential to the logarithm of the hydrogen ion concentration, was utilized to assess the

electrode's response behaviour. The Nernst equation was expressed as:

$$E = E_0 - \frac{2.303RT}{nF} pH ag{1}$$

Refer to (1), E denotes the electromotive force (emf) of the electrochemical cell, E_0 signifies the standard potential, R stands for the universal gas constant, T represents the absolute temperature, n indicates the number of electrons, and F denotes the Faraday constant [25-26].

III. RESULT

A. Surface Morphology by Digital Microscope and FESEM

1) Digital microscopy

Digital microscopy was employed to investigate surface morphology at the microscale. The obtained digital microscopy images in Fig. 3 for TiO₂, TiO₂-PANI EB and TiO₂-PANI ES material were deposited by the spin coating method at a similar magnification, 20x. TiO₂-PANI EB exhibited a more uniform distribution composite, in the DMF solvent. Conspicuously, TiO₂-PANI ES displayed an undissolved polyaniline salt base in the methanol solvent, revealing huge dark spots with a yellowish hue around the side that was believed interpreted as undissolved PANI ES.

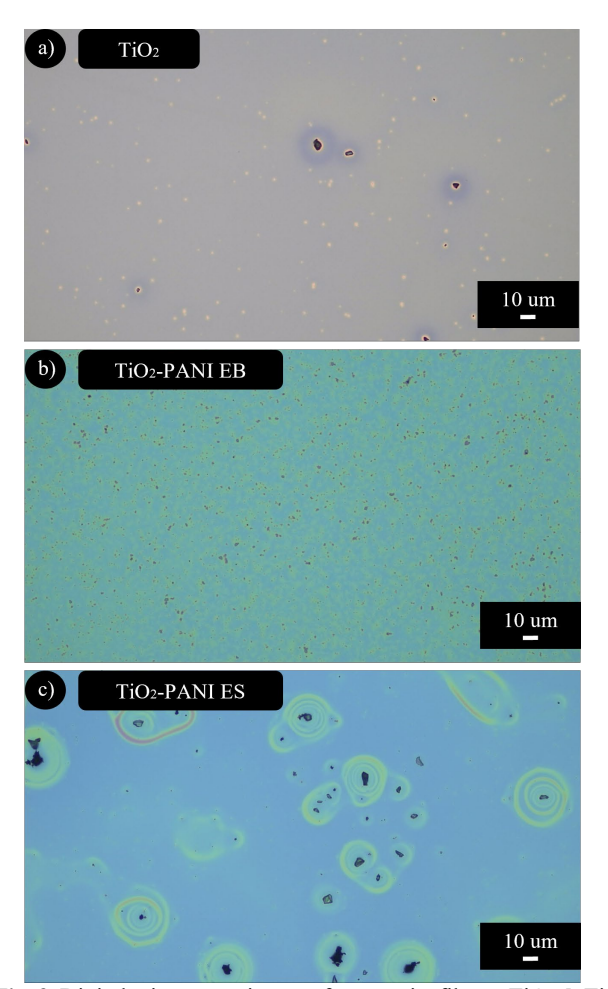


Fig. 3. Digital microscope image of composite films a TiO_2 , b TiO_2 -PANI EB and c TiO_2 -PANI ES.

2) FESEM

The FESEM analysis conducted at 50,000x magnification for all sensing layers revealed similar structural properties. From the observations in Fig. 4, it was observed that the uniform distribution of TiO₂, TiO₂-PANI EB and TiO₂-PANI ES composites on the surface of the ITO substrate exhibited an asymmetric shape. Additionally, the nanoparticles appeared to be uniformly dispersed across the substrate surface, contributing to the formation of a consistent and continuous thin film. Significantly, with the incorporation of polymer, the surface morphology showed an increase in nanoparticle size. The increase in particle size observed in the TiO₂-PANI composite is attributed to the polymer coating effect and possible nanoparticle aggregation induced by the polymer matrix, which alters the surface morphology compared to pristine TiO₂.

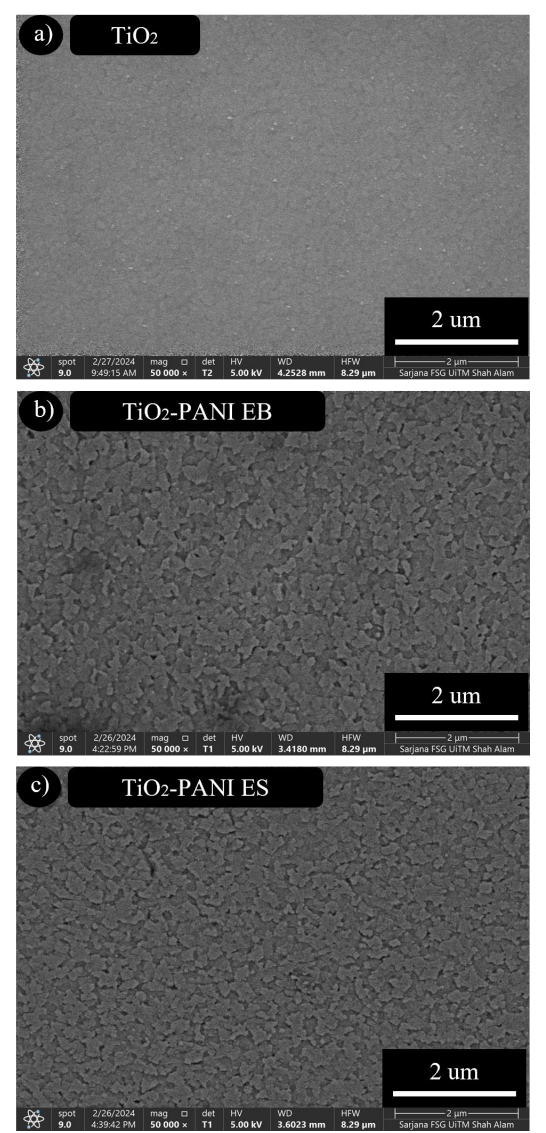


Fig. 4. FESEM images of composite films **a** TiO₂, **b** TiO₂-PANI EB and **c** TiO₂-PANI ES.

B. Contact Angle

The study conducted contact angle measurements using the sessile drop method, which involved placing a droplet of DI water on the material's surface and analyzing the angle formed between the droplet and the surface as shown in Fig. 5. As presented in Table II, the average contact angles of the sessile droplets dispensed at randomly deposited areas were calculated. TiO₂ alone exhibits a contact angle of 79.20°, TiO₂-PANI EB showed a higher contact angle at 92.70° compared to TiO₂-PANI ES at 87.57°. It can be concluded that the type of polymer influences the interfacial properties of the pH sensing layer. Specifically, it was observed that PANI EB exhibited hydrophobic properties, while PANI ES showed hydrophilic properties. These differences in interfacial behaviour were attributed to the distinct chemical compositions and surface properties of the polymers. An increase in contact angle could have affected the adhesion strength between the deposited film and the ITO substrate [20], [21], [27]. This study showed that the PANI EB polymer presented stronger adhesion to the ITO substrate surface. These findings had an impact on a stable sensing performance with less tendency to swell or peel during the EGFET measurement.

Due to its lower contact angle, the TiO_2 film was not pursued further in this study.

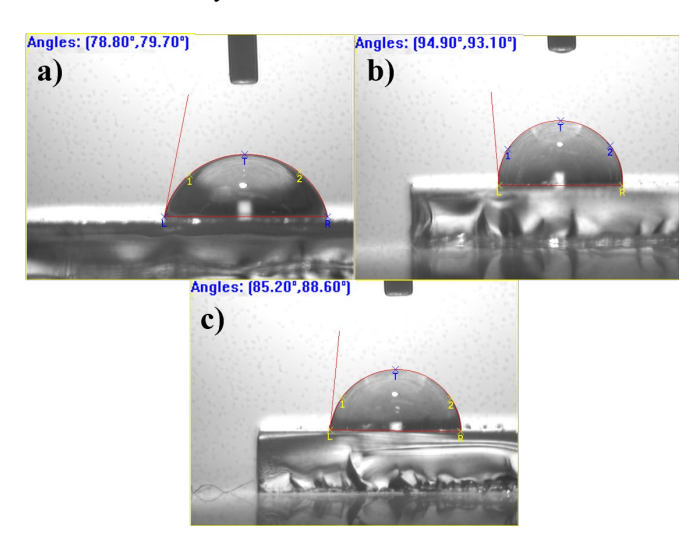


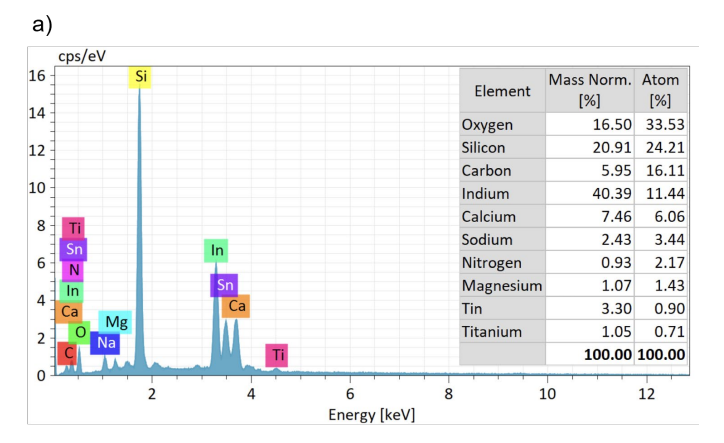
Fig. 5. Sessile drop on the surface of composite films **a** TiO_2 **b** TiO_2 -PANI EB and **c** TiO_2 -PANI ES.

TABLE II. AVERAGE OF CONTACT ANGLE TIO2-PANI-BASED FILMS

TiO ₂ -PANI-based film	Contact angle	
TiO ₂	79.20°	
TiO ₂ -PANI EB	92.70°	
TiO ₂ -PANI ES	87.57°	

C. EDX Analysis

The analysis of elemental composition in both TiO₂-PANIbased films was conducted using EDX measurements with an acceleration voltage of 20 kV. EDX analysis is crucial in confirming the elemental composition and uniform integration of TiO₂ and PANI in the composite film, which underpins its structural integrity and performance as a reliable pH sensing electrode. The atomic percentages representing elements from the ITO substrate, including silicon (Si), indium (In), tin (Sn), and oxygen (O), were observed in the EDX results as shown in Fig. 6. Additionally, based on previous research findings, the peak elements of carbon (C), nitrogen (N), and oxygen (O) were identified as part of the polymer PANI material [18], [28]. In Fig. 6a, the TiO₂-PANI EB sensing film exhibited a higher atomic percentage, indicating the presence of PANI elemental materials with carbon (C) at 16.11%, nitrogen (N) at 2.17%, and oxygen (O) at 33.53%. This observation aligns with expectations based on previous studies regarding the elemental composition of PANI EB. Contrastingly, in Fig. 6b, the TiO₂-PANI ES film showed a lower percentage of PANI elemental materials, with carbon (C) at 15.63%, nitrogen (N) at 2.12%, and oxygen (O) at 31.50%. The higher amount of PANI elements in the composite layer improved its conductivity significantly. The EDX analysis provided valuable insights into the elemental composition of the TiO₂-PANI-based films, highlighting differences in polymer PANI content between PANI EB and PANI ES films.



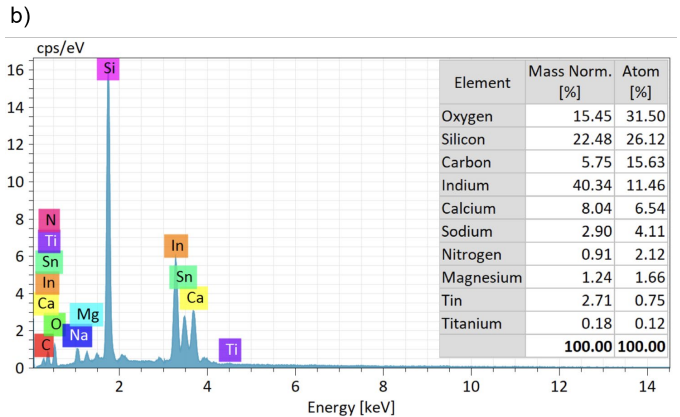


Fig. 6. Elemental composition analysis of TiO₂-PANI-based films on EDX **a** TiO₂-PANI EB and **b** TiO₂-PANI ES.

D. Hysteresis characteristic

Hysteresis measurement for TiO_2 -PANI EB and TiO_2 -PANI ES sensing electrode (SE) using EGFET setup connect to B1500A equipment implement acidic loop starting from pH level $7 \rightarrow 4 \rightarrow 7 \rightarrow 10 \rightarrow 7$ over 25 minutes. The hysteresis graph in Fig. 7 presents the SE performance comparing its hysteresis rate was found to be 17 mV and 40 mV respectively. The TiO_2 -PANI EB perform two times lower compared to TiO_2 -PANI ES. This demonstrates that the TiO_2 -PANI EB electrode has a significantly lower hysteresis. We believed this behavior arises due to ion exchange processes at the sensing membrane's surface, where delays in the sensor's response are dependent on the rate at which ions are absorbed or diffuse, particularly in regions with weak structural integrity within the sensing membrane [20], [27].

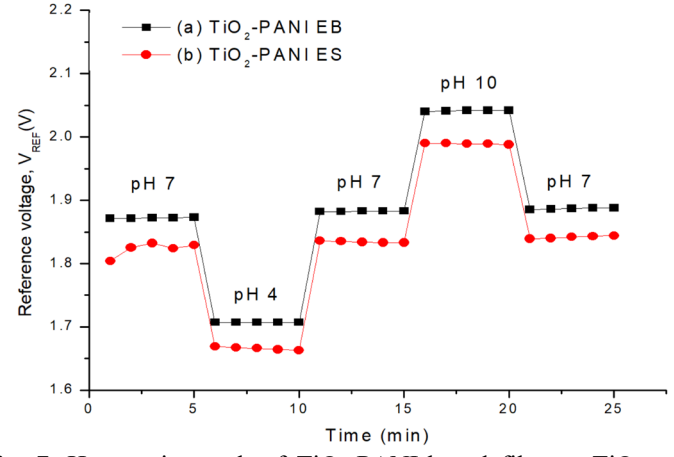


Fig. 7. Hysteresis graph of TiO₂-PANI-based films **a** TiO₂-PANI EB and **b** TiO₂-PANI ES tested in acidic loop.

E. Nernst response analysis of pH sensing electrode

TABLE III. NERNST RESPONSE OF TIO2-PANI-BASED FILMS

TiO ₂ -PANI-based film	Sensitivity (mV/pH)	Linearity
TiO ₂ -PANI EB	57.10	0.9995
TiO ₂ -PANI ES	46.24	0.9963

The result of the pH value and voltage reference are depicted in Fig. 8 The sensitivity and linearity of the TiO₂-PANI-based films were recorded in Table III. The drain-source current, I_{DS} was kept constant at 100 μA. The TiO₂-PANI EB shows the highest Nernst response at 57.10 mV/pH sensitivity and 0.9995 linearity, compared to TiO2-PANI ES, which demonstrated a lower result; at 46.24 mV/pH sensitivity and 0.9963 linearity. This study revealed that the polymer PANI EB enhanced the sensing performance of the pH sensor. The improvement in sensor response in terms of sensitivity and linearity was further supported by the contact angle result, indicating that TiO₂-PANI EB exhibited hydrophobic properties, confirming its strong adhesion between the ITO glass and deposited film. Manjakkal et al. suggested adding a factor to Equation (1), which was related to the electrode-solution interface reaction and the variations in the impedance of the Faradaic reaction that formed the electrochemical double layer (EDL) [26], [29]. The chemical reaction occurred between the surface of TiO₂-PANIbased films and the electrolyte in different pH buffer solutions.

The enhancement was also related to the EDX analysis, where the peak of PANI material in TiO₂-PANI EB was more dominant compared to TiO₂-PANI ES, allowing for an improvement in conductivity. In this case, the higher conductivity facilitated faster ion transport, which was highly beneficial in applications requiring rapid ion movement. Moreover, it ensured that even minor variations in pH resulted in detectable electrical changes at the EDL, consequently reducing noise interference during the EGFET measurement.

High conductivity implies efficient charge transfer, while strong adhesion ensures better contact between the sensing material and the electrode, both of which were crucial for efficient ion exchange. Overall, based on the results obtained in this study, it was believed that the improvement in conductivity and strong adhesion of the sensing films enhanced the ions (H⁺ and OH⁻) exchange process through (adsorption/diffusion), thus contributing to the overall pH sensor performance.

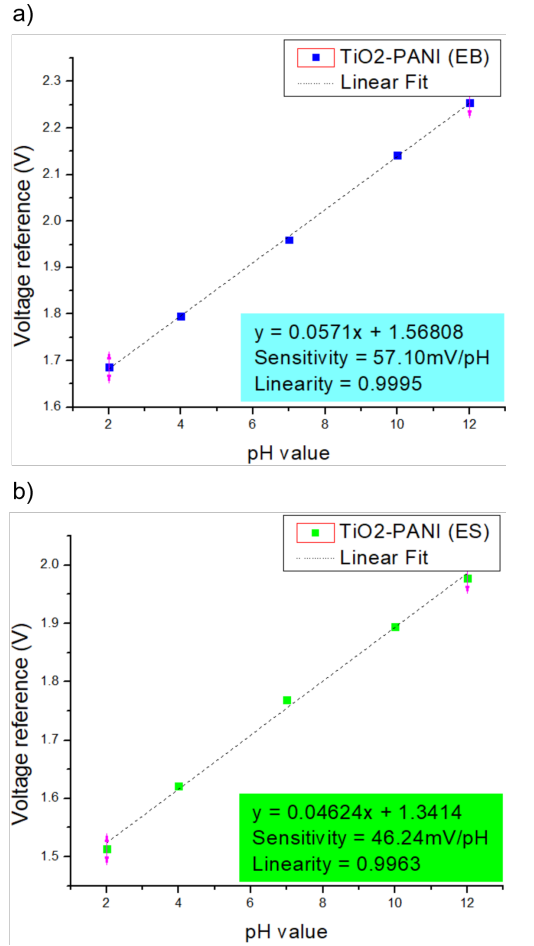


Fig. 8. Sensitivity and linearity of prepared TiO₂-PANI-based films output voltage vs. pH value.

IV. CONCLUSION

The study into composite TiO₂-PANI EB and TiO₂-PANI ES films using digital microscopy, FESEM analysis, contact angle

measurements, EDX analysis, hysteresis characteristic and Nernst response analysis revealed crucial insights into their performance as pH sensors. Digital microscopy highlighted the superior uniformity of TiO2-PANI EB compared to the undissolved regions in TiO2-PANI ES, affecting their morphology. FESEM analysis showed similar structural properties with uniform nanoparticle distribution contributing to thin film formation on ITO substrates. Contact angle measurements indicated that PANI EB's hydrophobicity led to stronger adhesion to the substrate, contributing to stable sensing performance. EDX analysis demonstrated higher PANI content in TiO₂-PANI EB, aligning with its enhanced conductivity and better sensor response as evidenced by lower hysteresis rate and Nernst response analysis, where TiO₂-PANI EB showed high sensitivity and linearity. These findings suggest that the choice of polymer PANI-based significantly influences the interfacial properties and overall performance of composite TiO₂-PANIbased films pH sensors, with selection of polymer PANI EB exhibiting significant advantages in terms of adhesion, conductivity and sensing performance. These improvements are directly linked to enhanced charge transfer and ion transport at the electrode electrolyte interface, which are critical for reliable electronic pH sensing. By relating material properties such as conductivity and adhesion to sensor output, this study demonstrate the importance of polymer selection in optimizing electronic device performance, aligning the study with the scope of electrical and electronic systems.

ACKNOWLEDGMENT

The authors would like to express their gratitude for the partial support received from the Ministry of Higher Education Malaysia through the Fundamental Research Grant Scheme (Project Code: FRGS/1/2021/TK0/UITM/02/50). They also acknowledge the invaluable technical assistance provided by the NANO ElecTronic Centre (NET) at the Faculty of Electrical Engineering and Instrumental Chemistry Lab I at the Faculty of Chemical Engineering, UiTM Shah Alam.

REFERENCES

- [1] C. W. Wang and T. M. Pan, "Structural properties and sensing performances of CoNxOy ceramic films for EGFET pH sensors," *Ceram Int*, vol. 47, no. 18, pp. 25440–25448, Sep. 2021, doi: 10.1016/j.ceramint.2021.05.266.
- [2] H. A. Khizir and T. A. H. Abbas, "Hydrothermal synthesis of TiO2 nanorods as sensing membrane for extended-gate field-effect transistor (EGFET) pH sensing applications," Sens Actuators A Phys, vol. 333, Jan. 2022, doi: 10.1016/j.sna.2021.113231.
- [3] B. K. Yadlapalli, H. Y. Chou, J. L. Chiang, and D. S. Wuu, "Morphological investigation and pH sensing properties of β-Ga2O3 EGFET-pH sensor," *Materials Science and Engineering: B*, vol. 300, Feb. 2024, doi: 10.1016/j.mseb.2023.117113.
- [4] T. M. Pan, C. H. Yang, and S. T. Pang, "Structural properties and sensing performance of Ni–Ti alloy films for extended-gate fieldeffect transistor pH sensors," *Mater Sci Semicond Process*, vol. 164, Sep. 2023, doi: 10.1016/j.mssp.2023.107639.
- [5] X. Zeng, W. Jiang, X. Jiang, G. I. N. Waterhouse, Z. Zhang, and L. Yu, "Stable Pb2+ ion-selective electrodes based on polyaniline-TiO2 solid contacts," *Anal Chim Acta*, vol. 1094, pp. 26–33, Jan. 2020, doi: 10.1016/j.aca.2019.10.008.
- [6] C. Chen, Y. Zhang, H. Gao, K. Xu, and X. Zhang, "Fabrication of Functional Super-Hydrophilic TiO 2 Thin Film for pH Detection," 2022, doi: 10.3390/chemosensors.

- [7] M. Nematzadeh, O. Nilsen, P. D. Häfliger, and V. A. L. K. Killi, "Investigation of the Atomic Layer Deposition of the Titanium Dioxide (TiO2) Film as pH Sensor Using a Switched Capacitor Amplifier," *Chemosensors*, vol. 10, no. 7, Jul. 2022, doi: 10.3390/chemosensors10070274.
- [8] S. Kailasa, M. Sai Bhargava Reddy, B. Geeta Rani, K. Venkateswara Rao, K. Deshmukh, and K. Kumar Sadasivuni, "Highly sensitive electrochemical volatile organic compound (Acetone) sensing based on TiO2 Nanocubes @Polyaniline nanostructure," *Inorg Chem Commun*, vol. 157, Nov. 2023, doi: 10.1016/j.inoche.2023.111420.
- [9] S. Nazari, M. S. Khiabani, R. R. Mokarram, H. Hamishehkar, Y. Chisti, and S. Tizchang, "Optimized formulation of polyaniline-pectin optical film sensor for pH measurement," *Materials Science and Engineering: B*, vol. 294, Aug. 2023, doi: 10.1016/j.mseb.2023.116517.
- [10] Y. Wu, X. Gao, and Y. Li, "Electrochemical sensors based on polyaniline nanocomposites for detecting Cd(II) in wastewater," *Int J. Electrochem Sci*, vol. 19, no. 3, Mar. 2024, doi: 10.1016/j.ijoes.2024.100519.
- [11] A. I. Alalawy, N. S. Zidan, M. Sakran, A. Y. Hazazi, E. S. Salama, and M. A. Alotaibi, "Enhancing bioelectricity generation in seaweed-derived microbial fuel cells using modified anodes with Fe2O3@AuNPs/PANI nanocomposites," *Biomass Bioenergy*, vol. 182, Mar. 2024, doi: 10.1016/j.biombioe.2024.107104.
- [12] C. Dawo, P. Krishnan Iyer, and H. Chaturvedi, "Carbon nanotubes/PANI composite as an efficient counter electrode material for dye sensitized solar cell," *Materials Science and Engineering: B*, vol. 297, Nov. 2023, doi: 10.1016/j.mseb.2023.116722.
- [13] B. Xu et al., "Electrospinning preparation of PAN/TiO2/PANI hybrid fiber membrane with highly selective adsorption and photocatalytic regeneration properties," Chemical Engineering Journal, vol. 399, Nov. 2020, doi: 10.1016/j.cej.2020.125749.
- [14] M. Beygisangchin, S. A. Rashid, S. Shafie, A. R. Sadrolhosseini, and H. N. Lim, "Preparations, properties, and applications of polyaniline and polyaniline thin films—a review," *Polymers (Basel)*, vol. 13, no. 12, Jun. 2021, doi: 10.3390/polym13122003.
- [15] M. Waqas et al., "Polyaniline/polyvinylpyrrolidone nanofibers via nozzle-free electrospinning," J Appl Polym Sci, vol. 140, no. 43, Nov. 2023, doi: 10.1002/app.54586.
- [16] J. Qiao et al., "Electrochemical properties of aluminum ion batteries with emeraldine base polyaniline as cathode material," Journal of Electroanalytical Chemistry, vol. 929, Jan. 2023, doi: 10.1016/j.jelechem.2022.117102.
- [17] M. Morsy, A. Elzwawy, A. I. Abdel-Salam, M. M. Mokhtar, and A. B. El Basaty, "The humidity sensing characteristics of PANI-titania nanotube-rGO ternary nanocomposite," *Diam Relat Mater*, vol. 126, Jun. 2022, doi: 10.1016/j.diamond.2022.109040.
- [18] J. G. Shin, C. S. Park, E. Y. Jung, B. J. Shin, and H. S. Tae, "Synthesis of a polyaniline nanoparticle using a solution plasma process with an Ar gas bubble channel," *Polymers (Basel)*, vol. 11, no. 1, Jan. 2019, doi: 10.3390/polym11010105.
- [19] B. Fryczkowska, Z. Piprek, M. Sieradzka, R. Fryczkowski, and J. Janicki, "Preparation and Properties of Composite PAN/PANI Membranes," Int. J. Polym. Sci., vol. 2017, 2017, doi: 10.1155/2017/3257043.
- [20] D. V. Antonov, A. G. Islamova, and P. A. Strizhak, "Hydrophilic and Hydrophobic Surfaces: Features of Interaction with Liquid Drops," Sep. 01, 2023, Multidisciplinary Digital Publishing Institute (MDPI). doi: 10.3390/ma16175932.
- [21] E. K. Kerstner, S. R. Kunst, L. V. R. Beltrami, M. R. O. Vega, L. C. Scienza, and C. De Fraga Malfatti, "Anticorrosive performance of commercial nanoceramic coatings on AISI 1010 steel," *Materials Research*, vol. 17, no. 6, pp. 1497–1506, Nov. 2014, doi: 10.1590/1516-1439.263514.
- [22] F. Sotoudeh, S. M. Mousavi, N. Karimi, B. J. Lee, J. Abolfazli-Esfahani, and M. K. D. Manshadi, "Natural and synthetic superhydrophobic surfaces: A review of the fundamentals, structures, and applications," Apr. 01, 2023, *Elsevier B.V.* doi: 10.1016/j.aej.2023.01.058.
- [23] F. Wang, M. Xiang, and W. Yang, "Effects of contact angle hysteresis on frosting and defrosting characteristics on vertical superhydrophobic surfaces," *Appl Therm Eng*, vol. 236, Jan. 2024, doi: 10.1016/j.applthermaleng.2023.121881.

- [24] Sensors Council, Annual IEEE Computer Conference, Md. IEEE Sensors Conference 12 2013.11.03-06 Baltimore, and Md. IEEE Sensors Conference 12 2013.11.04-06 Baltimore, IEEE sensors, 2013 3-6 Nov. 2013, Baltimore, Maryland, USA; proceedings; the 12th IEEE Sensors Conference.
- [25] P. Kurzweil, "Metal oxides and ion-exchanging surfaces as pH sensors in liquids: State-of-the-art and outlook," Jun. 2009. doi: 10.3390/s90604955.
- [26] L. Manjakkal, D. Szwagierczak, and R. Dahiya, "Metal oxides based electrochemical pH sensors: Current progress and future perspectives," Apr. 01, 2020, Elsevier Ltd. doi: 10.1016/j.pmatsci.2019.100635.
- [27] D. Shantini, I. Nainggolan, T. I. Nasution, M. N. Derman, R. Mustaffa, and N. Z. Abd Wahab, "Hexanal Gas Detection Using Chitosan Biopolymer as Sensing Material at Room Temperature," J Sens, vol. 2016, 2016, doi: 10.1155/2016/8539169.
- [28] D. K. Pyne, S. Chatterjee, S. Pramanik, and A. Halder, "Temperature-induced photoluminescence amplification of graphene oxide-polyaniline composite through interaction modulated charge transfer," *Mater Chem Phys*, vol. 318, p. 129241, May 2024, doi: 10.1016/j.matchemphys.2024.129241.
- [29] S. Ravichandran, C. Thiagarajan, and P. S. Kumar, "pH Sensitivity Estimation in Potentiometric Metal Oxide pH Sensors Using the Principle of Invariance," *International Journal of Chemical Engineering*, vol. 2021, 2021, doi: 10.1155/2021/5551259.